Robust Indirect-Type Iterative Learning Control Design for Batch Processes with State Delay, Non-repetitive Uncertainties and Disturbances

Hongfeng Tao, Junyu Wei [*], Shoulin Hao[†], Wojciech Paszke[‡], Eric Rogers[§]

13.10.2024

Abstract

Iterative Learning Control (ILC) is renowned for its capability to achieve precise tracking control for systems with repetitive actions at a fixed time interval. However, pursuing the dual objective of high-precision tracking and rapid convergence is a persistent challenge in the field of learning control. To address this problem, a novel ILC method is designed for a class of discrete-time linear systems subject to non-repetitive disturbances in this paper. Particularly, the updating term in ILC is constructed inspired by the principle of sliding mode control (SMC), which results in the learning process being divided into two distinct stages: a rapid reaching stage and a slow sliding stage. As a result, a balance between convergence speed and tracking performance can be ensured via the proposed ILC method. In addition, to attenuate the effects of non-repetitive disturbances, the

[*]Key Laboratory of Advanced Process Control for Light Industry of Ministry of Education, Jiangnan University, Wuxi, 214122, PR China, CONTACT Hongfeng Tao. Email: taohongfeng@hotmail.com

[†]Key Laboratory of Intelligent Control and Optimization for Industrial Equipment of Ministry of Eduction, and the Institute of Advanced Control Technology, Dalian University of Technology, Dalian, 116024, China

[‡]Institute of Automation, Electronic and Electrical Engineering, University of Zielona Góra, ul. Szafrana 2, 65-516 Zielona Góra, Poland

[§]School of Electronics and Computer Science, University of Southampton, Southampton SO17 1BJ, United Kingdom

disturbance compensation mechanism is integrated into the proposed ILC method. Moreover, the optimal value of the learning gain can be determined using the predicted root mean square (RMS) errors of subsequent iterations, eliminating the need for additional tuning actions. Finally, simulation examples are provided to validate the effectiveness and superiority of the proposed new ILC method.

Keywords: Batch processes; iterative learning control; time delay; time- and batch-varying uncertainties; generalized extended state observer.

1 Introduction

Batch processes are a set of typical repetitive operations mainly used in the manufacturing of products, e.g., cooling crystallization [3, 6], semiconductor production [14], industrial injection molding [1, 5, 12, 17]. Many control methods have been developed for batch processes to meet product requirements and improve system performance, and it remains a topic of considerable interest.

Processing of each batch entry occurs over a finite and fixed time interval, and there is an elapsed time between the completion of the processing of one batch and the start of the next. Consequently, it is an application area for iterative learning control (ILC). In this form of control, data from previous batches is used to update the control signal for application during the processing of the subsequent trial. The aim is to sequentially improve performance from trial to trial and also regulate the dynamics along a trial. For ILC applied to batch processing, please refer to the survey papers, e.g., [11, 15] and references therein.

Uncertainties, as a result, e.g., of modeling assumptions and external disturbances contribute to the dynamics of batch processes. Although robust ILC designs have been developed for this general application area, most only consider repetitive uncertainties and disturbances. However, industrial batch processes are often affected by nonrepetitive disturbances such as time-varying uncertainties, or trial-dependent random disturbances.

One way of addressing these issues is to design robust ILC laws with a feedforward-feedback control structure. Several methods for this type of design have been developed. One of these is to treat ILC as a two-dimensional (2D) linear system with one direction of information propagation from batch to batch and the other temporal propagation within a batch. Recent work includes [18] and a generalized extended state observer (GESO) design [2], but these designs cannot achieve perfect tracking.

Time delays in batch processes, e.g., signal transmission time between sensors, actuators, and controllers, network delay, etc., are also inevitable and may lead to the deterioration of control performance or even system instability. Also, they make the analysis of disturbance rejection more difficult. Therefore, how to compensate for the time delays and deliver improved performance with disturbance rejection methods is particularly important. For example, [13] developed an iterative learning fault-tolerant control strategy for enhancing the robust performance of batch processes with uncertain dynamics and state delays using frequency domain analysis.

As an alternative to direct-type ILC designs, indirect-type ILC designs have been developed, with the possible advantage that the feedback and ILC parts can be designed relatively independently. The concept of indirect-type ILC was first reported in the survey paper [15]. The most obvious difference with direct-type ILC is that the latter directly acts on the input of the controlled system, updates the input on each trial, and is a one-step design. In indirect ILC a feedback control loop for stability and robustness is designed, termed the inner control loop, and then an ILC law is used to update, e.g., the set-point for the inner loop to enforce trial-to-trial error convergence. The outer loop acts as a supervisor or optimizer and does not change the control structure of the inner loop.

By employing an active disturbance rejection control scheme in the inner loop, a proportional (P-type) set-point ILC was developed in [1], such that the time- and batch-varying uncertainties can be significantly suppressed. For batch processes with output delay suffering from nonrepetitive uncertainties and disturbances, a predictive state observer-based set-point learning control was presented in [6] to realize batch optimization. In this paper, a controller is developed for each trial when model uncertainty and disturbances are present. This inner feedback control loop regulates the dynamics along a trial. The controller is GESO based state action combined with proportional plus integral (PI) action applied to the trial error. Next, an ILC law is developed that updates the set-point command of the inner-loop control structure to enforce trial-to-trial error convergence. The main contributions of this paper are:

- An efficient indirect-type ILC scheme is developed for batch processes with state delays and time-varying uncertainties, significantly improving the tracking performance against nonrepetitive disturbances compared with the recently developed direct-and indirect-type ILC from the initial batch.

- The design of the inner loop feedback system can be undertaken using a

tractable linear matrix inequality (LMI) condition, and the ILC design for set-point tracking does not affect the structure of the closed-loop.

- Both delay-independent and delay-dependent sufficient conditions are established to ensure the convergence of tracking error and robust stability along the trial, respectively.

Notation. $\mathbb{Z}_+ = \{1, 2, \cdots\}$, $\mathbb{Z}_N = \{0, 1, 2, \cdots, N\}$ for any $N \in \mathbb{Z}_+$; I and 0 denote identity and null matrices with compatible dimensions, respectively; $P \succ 0$ (or $P \prec 0$) denotes the symmetric positive (negative) definite property of P, respectively, $P \succeq 0$ (or $P \preceq 0$) denotes the symmetric positive (negative) semi-definite property of P. $(*)$ denotes block entries in symmetric matrices. The symbol $\text{diag}\{\cdot\}$ denotes a block-diagonal matrix and $\text{sym}\{X\} = X + X^T$. $\|\cdot\|$ denotes the Euclidean vector norm or the induced matrix norm, and for a vector f_k, with k denoting the trial number, $\delta f_k(t+1) = f_k(t) - f_{k-1}(t)$ denotes the difference on two successive trials. In keeping with the ILC literature, trial is used instead of batch in the rest of this paper.

The following lemmas are used in this paper to prove the new results.

Lemma 1 *[19] Given matrices X and Y with compatible dimensions, the following inequality holds for any scalar $\varepsilon > 0$ and matrix Δ that satisfies $\Delta^T\Delta \preceq \text{I}$*

$$\text{sym}\{X\Delta Y\} \preceq \varepsilon XX^T + \varepsilon^{-1}Y^TY.$$

Lemma 2 *[7] Consider the following system over $k \in \mathbb{Z}_+$ and $t \in \mathbb{Z}_N$*

$$x_{k+1}(t) = \Omega_k(t)x_k(t) + u_k(t), \tag{1}$$

where $\Omega_k(t) \in \mathbb{R}^{p\times p}$ is the mapping matrix, $x_k(t) \in \mathbb{R}^p$ and $u_k(t) \in \mathbb{R}^p$ denote the state and external input vectors, respectively, and the initial state vector $x_0(t)$ and $u_k(t)$ are bounded, i.e., $\beta_{x_0} = \max\limits_{t\in\mathbb{Z}_N}\|x_0(t)\| < \infty$ and $\beta_u(t) = \sup\limits_{k\in\mathbb{Z}_+}\|u_k(t)\| < \infty$. Then, there exists upper bounds $\beta_x(t) > \beta_{x_{\text{sup}}}(t) \geq 0$ satisfying $\sup\limits_{k\in\mathbb{Z}_+}\|x_k(t)\| \leq \beta_x(t)$ and $\limsup\limits_{k\to\infty}\|x_k(t)\| \leq \beta_{x_{\text{sup}}}(t)$ for the system in (1) if $\|\Omega_k(t)\| \leq \chi < 1$ holds for any $k \in \mathbb{Z}_+$ and $t \in \mathbb{Z}_N$.

2 Preliminaries

The specification and design of ILC laws can be undertaken using two general approaches: direct and indirect. In the former, the aim is to design

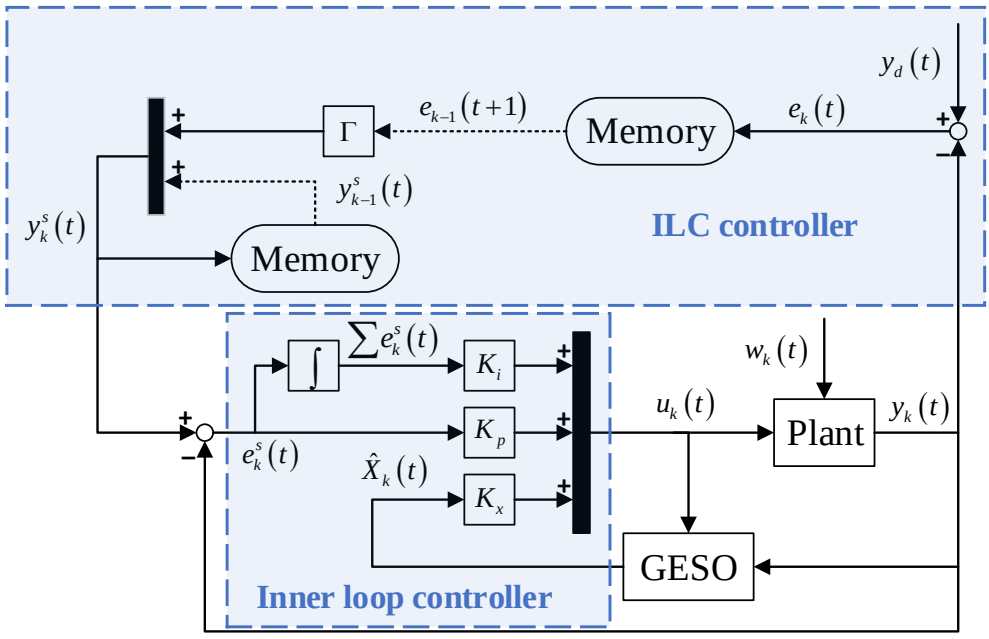

Figure 1: Structure of the new indirect-type ILC system.

the control law to simultaneously enforce trial-to-trial error convergence and regulate the dynamics produced on any trial. Several design methods have been developed, one of which is to use the 2D systems structure of the dynamics, i.e., information propagation from trial to trial (in k) and along a trial (in t). In the literature, this approach is sometimes referred to as direct design, and many design algorithms have been developed, some through experimental validation and implementation, see, e.g., [10] which, in turn, cites the original work for the application and design method used. Difficulties can, however, arise, particularly in cases when a dynamic control law is needed together with a robust design and disturbance rejection due to the complexity of the resulting design.

As an alternative, indirect ILC design allows for using two loops, inner and outer, each of which can be designed separately. In this approach, the inner loop can be designed using standard approaches, such as $\mathcal{H}_\infty$ methods. Then, the outer ILC loop can be designed to ensure trial-to-trial error convergence. Figure 1 shows the indirect-type ILC scheme developed in this paper, which consists of a local feedback controller, the inner loop, and an ILC law, the outer loop.

This paper develops an indirect robust ILC design for discrete-time batch processes with state delay, time-varying uncertainty and disturbances. One

option for ILC for discrete dynamics is to use the lifted setting, i.e., the values of variables over the trial length are assembled into a column vector. Then, the trial-to-trial error updating is described using a standard linear systems model. If necessary, a feedback control loop is first designed to regulate the trial dynamics (in t), and then the ILC law is designed for the resulting dynamics.

The lifted model could result in computations with very large dimensional matrices in the presence of delays and disturbances. Moreover, for robust control design, at least some of the matrices could have block entries that are products of the nominal model matrices and those describing the uncertainty, creating serious design difficulties. The design developed in this paper first develops an inner loop controller to regulate the along-the-trial dynamics and then uses the repetitive process setting to design the outer (ILC) loop. In this way, the very large dimensional matrices problem does not arise.

In particular, the dynamics of the systems considered are described by the following state-space model over $k \in \mathbb{Z}_+$, $t \in \mathbb{Z}_N$

$$\begin{aligned} x_k(t+1) =& A_k(t)x_k(t) + A_{h,k}(t)x_k(t-h) + B_k(t)u_k(t) + B_w w_k(t), \\ y_k(t) =& Cx_k(t), \end{aligned} \tag{2}$$

where $N \in \mathbb{Z}_+$ is the fixed and finite trial length; $x_k(t) \in \mathbb{R}^{n_x}$, $u_k(t) \in \mathbb{R}^{n_u}$ and $y_k(t) \in \mathbb{R}^{n_y}$ denote, respectively, the state, input and output vectors, and $w_k(t) \in \mathbb{R}^{n_w}$ represents the external load disturbance vector. Also, h is an unknown but bounded state delay satisfying $h \in \mathbb{Z}_{\bar{h}}$, where $\bar{h}$ is a known upper bound. Assume that $x_k(t) = x_0$ for $t \leq 0$, x_0 is the identical initial state vector for each trial satisfying $\|x_0\| \leq \beta_{x_0} < \infty$, $A_k(t) = A + \Delta A_k(t)$, $A_{h,k}(t) = A_h + \Delta A_{h,k}(t)$, and $B_k(t) = B + \Delta B_k(t)$ are time- and batch-varying system matrices, where $\Delta A_k(t) = E\Delta_k(t)F_a$, $\Delta A_{h,k}(t) = E\Delta_k(t)F_h$, $\Delta B_k(t) = E\Delta_k(t)F_b$, and $\{E, F_a, F_h, F_b\}$ are known/estimated constant matrices that characterize the structure of uncertainties and their corresponding weights. Finally, $\Delta_k(t)$ represents the time- and batch-varying uncertainty satisfying $\Delta_k^T(t)\Delta_k(t) \preceq \mathrm{I}$. Without loss of generality, it is assumed that the pair (A, B) is controllable and the pair (C, A) is observable. Also, the matrix C is full row rank and therefore its right inverse $C^T(CC^T)^{-1}$ exists.

Given a user-specified reference trajectory $y_d(t)$ satisfying $\|y_d(t)\| \leq \beta_r < \infty$ and define the tracking error as $e_k(t) = y_d(t) - y_k(t)$. The zero error requirement cannot be satisfied for batch-varying uncertainties and disturbances. An alternative is required to achieve bounded convergence of tracking error, i.e.,

$$\sup_{k\geq 0} \|e_k(t)\| \leq \beta_e, \ \limsup_{k\to\infty} \|e_k(t)\| \leq \beta_{e_{\sup}}, \tag{3}$$

where $\beta_e > \beta_{e_{\sup}} \geq 0$ are finite bounds. Also, the control input and process state vectors in (2) should be bounded, i.e.,

$$\sup_{k\geq 0} \max_{t\in\mathbb{Z}_{N-1}} \|u_k(t)\| \leq \beta_u < \infty, \ \sup_{k\geq 0} \max_{t\in\mathbb{Z}_N} \|x_k(t)\| \leq \beta_x < \infty, \tag{4}$$

where $\beta_u \geq 0$ and $\beta_x \geq 0$ are finite upper bounds. The following assumption is also used in the proofs of the new results in this paper.

Assumption 1 *[7] It is assumed that $A_k(t)$, $A_{h,k}(t)$, $B_k(t)$ and $w_k(t)$ are bounded for any $k \in \mathbb{Z}_+$ and $t \in \mathbb{Z}_N$, i.e.,*

$$\begin{aligned} &\sup_{k\geq 0} \max_{t\in\mathbb{Z}_N} \|A_k(t)\| \leq \beta_A, \ \sup_{k\geq 0} \max_{t\in\mathbb{Z}_N} \|A_{h,k}(t)\| \leq \beta_{A_h}, \\ &\sup_{k\geq 0} \max_{t\in\mathbb{Z}_N} \|B_k(t)\| \leq \beta_B, \ \sup_{k\geq 0} \max_{t\in\mathbb{Z}_N} \|w_k(t)\| \leq \beta_w, \end{aligned} \tag{5}$$

where $\beta_A \geq 0$, $\beta_{A_h} \geq 0$, $\beta_B \geq 0$ and $\beta_w \geq 0$ are finite upper bounds.

By lumping the process uncertainties, external disturbance, and time delay into a total disturbance, the process description in (2) becomes

$$\begin{aligned} x_k(t+1) =& Ax_k(t) + Bu_k(t) + d_k(t), \\ y_k(t) =& Cx_k(t). \end{aligned} \tag{6}$$

where $d_k(t) = \Delta A_k(t)x_k(t) + \Delta A_{h,k}(t)x_k(t-h) + \Delta B_k(t)u_k(t) + B_w w_k(t)$. It can be seen that $d_k(t)$ is in fact dependent on the state variable of the process. To estimate the total disturbance $d_k(t)$ for feedforward compensation, an augmented system description for the system in (6) is given below by treating $d_k(t)$ as an extended state vector

$$\begin{aligned} X_k(t+1) =& \hat{A}X_k(t) + \hat{B}u_k(t) + \hat{D}\Delta d_k(t+1), \\ y_k(t) =& \hat{C}X_k(t), \end{aligned} \tag{7}$$

where $X_k(t) = [x_k^T(t) \quad d_k^T(t)]^T$, and $\Delta d_k(t+1) = d_k(t+1) - d_k(t)$ denotes the difference of the total disturbance along the time direction, at sample instants t and $t+1$, and

$$\hat{A} = \begin{bmatrix} A & \mathrm{I} \\ 0 & \mathrm{I} \end{bmatrix}, \hat{B} = \begin{bmatrix} B \\ 0 \end{bmatrix}, \hat{C} = \begin{bmatrix} C & 0 \end{bmatrix}, \hat{D} = \begin{bmatrix} 0 \\ \mathrm{I} \end{bmatrix}.$$

Using the augmented system in (7), the following GESO is designed to estimate the system state and disturbance simultaneously

$$\hat{X}_k(t+1) = \hat{A}\hat{X}_k(t) + \hat{B}u_k(t) + L[y_k(t) - \hat{C}\hat{X}_k(t)], \tag{8}$$

where $\hat{X}_k(t) = [\hat{x}_k^T(t) \quad \hat{d}_k^T(t)]^T$, $\hat{x}_k(t)$ and $\hat{d}_k(t)$ are the estimates of $x_k(t)$ and $d_k(t)$, respectively, and L is the observer gain to be determined. Next, define the set-point tracking error as

$$e_k^s(t) = y_k^s(t) - y_k(t), \tag{9}$$

where $y_k^s(t)$ is the set-point and will be iteratively updated by the outer loop ILC law. It is pointed out that $y_1^s(t) = y_d(t), \forall t \in \mathbb{Z}_N$, i.e., the set-point of the initial tiral is the reference trajectory. Steady-state tracking error reduction to the maximum extent possible on each trial is a desirable design objective. Consequently, the integral of the set-point tracking error is introduced as an additional state vector in the design of the local controller to reduce the steady-state tracking error. Also, introduce the notation $\sum e_k^s(t) = \sum_{i=0}^{t} e_k^s(i)$ for shorthand and it follows that $\sum e_k^s(t) = \sum e_k^s(t-1) + e_k^s(t)$.

The inner loop implements the following control law based on the observed extended state vector and set-point tracking error on each trial

$$u_k(t) = K_x \hat{X}_k(t) + K_p e_k^s(t) + K_i \sum e_k^s(t), \tag{10}$$

where $K_x = [k_x \quad k_d]$, K_p and K_i are matrices to be designed. On any trial k, the matrix K_x implements state feedback action, and K_p and K_i proportional plus integral (PI) action based on the set-point error on this trial.

3 Control design

3.1 Inner loop

The subscript k is not relevant to the design of the controller and the stability analysis of the inner loop controlled dynamics, so it is omitted from the variables in this section.

Applying the control law (10) to the system in (2) and the GESO in (8) results in the following description of the controlled dynamics

$$\begin{aligned} \mathcal{X}(t+1) =& \mathcal{A}(t)\mathcal{X}(t) + \mathcal{A}_h(t)\mathcal{X}(t-h) + \mathcal{B}_w w(t), \\ y(t) =& \mathcal{C}\mathcal{X}(t), \end{aligned} \tag{11}$$

where

$$
\begin{aligned}
\mathcal{X}(t) =&[x^T(t) \quad \hat{X}^T(t) \quad \sum e^T(t-1)]^T, \mathcal{A}(t) = \mathcal{A} + \mathcal{E}\Delta(t)\mathcal{F}_1,\\
\mathcal{A}_h(t) =&\mathcal{A}_h + \mathcal{E}\Delta(t)\mathcal{F}_h, \mathcal{C} = [C \quad 0 \quad 0], \mathcal{A} = A_1 + B_1K + L_1C_1,\\
B_1 =&[B^T \quad \hat{B}^T \quad 0]^T, K = [-K_{pi}C \quad K_x \quad K_i],\\
L_1 =&[0 \quad L^T \quad 0]^T, C_1 = [C \quad -\hat{C} \quad 0], K_{pi} = K_p + K_i,\\
\mathcal{E} =&[E^T \quad 0 \quad 0]^T, \mathcal{F}_1 = \mathcal{F}_a + F_bK, \mathcal{F}_a = [F_a \quad 0 \quad 0], \mathcal{F}_h = [F_h \quad 0 \quad 0],\\
A_1 =& \begin{bmatrix} A & 0 & 0 \\ 0 & \hat{A} & 0 \\ -C & 0 & \mathrm{I} \end{bmatrix}, \mathcal{A}_h = \begin{bmatrix} A_h & 0 & 0 \\ 0 & 0 & 0 \\ 0 & 0 & 0 \end{bmatrix}, \mathcal{B}_w = \begin{bmatrix} B_w \\ 0 \\ 0 \end{bmatrix}.
\end{aligned}
$$

The following result in the $\mathcal{H}_\infty$ setting characterizes robust stability in the along the trial direction.

Theorem 3.1 *Given an $\mathcal{H}_\infty$ control performance γ_{pi}, the controlled system described by (11) is robustly stable for any state delay h satisfying $h \in \mathbb{Z}_{\bar{h}}$, where $\bar{h}$ is a known upper bound, if there exist matrices $W_i \succ 0, i = 1, \cdots, 4$, Z_K, Z_L and a scalar $\varepsilon > 0$, such that the following LMI is feasible*

$$
\begin{bmatrix}
\varphi_{11} & \varphi_{12} & \varphi_{13} & \varphi_{14} & \mathcal{B}_w & 0 & 0 \\
(*) & \varphi_{22} & \varphi_{23} & \varphi_{24} & \bar{h}\mathcal{B}_w & 0 & 0 \\
(*) & (*) & \varphi_{33} & W_2 & 0 & W_2C_2^T & \varphi_{37} \\
(*) & (*) & (*) & \varphi_{44} & 0 & 0 & \varphi_{47} \\
(*) & (*) & (*) & (*) & -\gamma_{pi}\mathrm{I} & 0 & 0 \\
(*) & (*) & (*) & (*) & (*) & -\gamma_{pi}\mathrm{I} & 0 \\
(*) & (*) & (*) & (*) & (*) & (*) & -\varepsilon\mathrm{I}
\end{bmatrix} \prec 0, \tag{12}
$$

where $\varphi_{11} = -W_1 + \varepsilon\mathcal{E}\mathcal{E}^T$, $\varphi_{12} = \varepsilon\bar{h}\mathcal{E}\mathcal{E}^T$, $\varphi_{13} = A_1W_2 + B_1Z_K + Z_L$, $\varphi_{14} = \mathcal{A}_hW_2$, $\varphi_{22} = -W_2 + \varepsilon\bar{h}^2\mathcal{E}\mathcal{E}^T$, $\varphi_{23} = \bar{h}\varphi_{13} - \bar{h}W_2$, $\varphi_{24} = \bar{h}\varphi_{14}$, $\varphi_{33} = -W_4 - W_2$, $\varphi_{37} = (\mathcal{F}_aW_2 + F_bZ_K)^T$, $\varphi_{44} = -W_3 + W_4 - W_2$, $\varphi_{47} = (\mathcal{F}_hW_2)^T$. Moreover, if the LMI (12) is feasible, the matrices in the control law (10) can be obtained by the following parameterization

$$
L_1 = Z_LW_2^{-1}C_1^T(C_1C_1^T)^{-1}, \ [-K_{pi}C \quad K_x \quad K_i] = Z_KW_2^{-1}. \tag{13}
$$

Proof 1 *Consider the following Lyapunov-Krasovskii function*

$$
V_x[\mathcal{X}(t)] = \mathcal{X}^T(t)P_1\mathcal{X}(t) + \sum_{i=t-h}^{t-1}\mathcal{X}^T(i)(P_1-P_2)\mathcal{X}(i) + \bar{h}\sum_{j=-\bar{h}}^{-1}\sum_{i=t+j}^{t-1}\sigma^T(i)P_3\sigma(i),
$$

where $\sigma(i) = \mathcal{X}(t+1) - \mathcal{X}(t)$, $P_1 \succ P_2 \succ 0$ *and* $P_3 \succ 0$. *Next, calculate the difference of* $V_x[\mathcal{X}(t)]$ *at* $t+1$ *and* t *and define the following cost function for analysis*

$$V_x[\mathcal{X}(t+1)] - V_x[\mathcal{X}(t)] < -\left(\gamma_{pi}^{-1}\|e(t)\|_2^2 - \gamma_{pi}\|w(t)\|_2^2\right). \tag{14}$$

Since the reference trajectory does not affect the stability analysis of the closed-loop system, $e(t) = -Cx(t) = -\mathcal{C}\mathcal{X}(t)$ *results on setting* $y_d(t) = 0$. *Also, by substituting* (11) *into* (14), *it follows that*

$$\zeta^T(t)(\Lambda_1^T P_1 \Lambda_1 + \bar{h}^2 \Lambda_2^T P_3 \Lambda_2 + \gamma_{pi}^{-1} C_2^T C_2 + \Upsilon)\zeta(t) \prec 0, \tag{15}$$

where

$$\begin{aligned}
\zeta(t) =& [\mathcal{X}^T(t) \quad \mathcal{X}^T(t-h) \quad w^T(t)]^T, \Lambda_1 = [\mathcal{A}(t) \quad \mathcal{A}_h(t) \quad \mathcal{B}_w],\\
\Lambda_2 =& [\mathcal{A}(t) - \mathrm{I} \quad \mathcal{A}_h(t) \quad \mathcal{B}_w], C_2 = [\mathcal{C} \quad 0 \quad 0],\\
\Upsilon =& \begin{bmatrix} -P_2 - P_3 & P_3 & 0 \\ (*) & -P_1 + P_2 - P_3 & 0 \\ (*) & (*) & -\gamma_{pi}\mathrm{I} \end{bmatrix}.
\end{aligned}$$

Define $P_1 = W_1^{-1}$, $P_3 = W_2^{-1}$, $P_2 = W_2 W_4 W_2$, $K = Z_K W_2^{-1}$, $L_1 C_1 = Z_L W_2^{-1}$. *Applying Schur's complement lemma and Lemma 1 to the LMI in* (12), *and then pre- and post-multiplying* (12) *by* $\mathrm{diag}\{\mathrm{I}, \mathrm{I}, P_3, P_3, \mathrm{I}, \mathrm{I}\}$, *it follows that the inequality in* (15) *holds.*

Remark 1 *Note that similar to the most Lyapunov-Krasovskii based stability analysis, the LMI condition* (12) *established in Theorem 3.1 is only a sufficient one whose feasibility may be affected by various factors including parameter matrices, time delay and uncertainty bound. In other words, the feasibility of the established sufficient condition is case-dependent. This is the same to almost all LMI based stability conditions. Even if the LMI constraints* (12) *were found infeasible, the controller gains can still be determined using other methods such as pole placement [1] and PID tuning [5]. In this paper, the feasibility of LMI condition is verified by Examples 1 and 2.*

Optimal $\mathcal{H}_\infty$ control performance follows by using the following optimization problem to determine the control law matrices

$$\begin{array}{ll} \min & \gamma_{pi} \\ s.t. & (12) \end{array} \tag{16}$$

3.2 Outer Loop

Using (2), (8) and (10) results in

$$\begin{aligned} \mathcal{X}_k(t+1) =& \mathcal{A}_k(t)\mathcal{X}_k(t) + \mathcal{A}_{h,k}(t)\mathcal{X}_k(t-h) + \mathcal{B}_k(t)y_k^s(t) + \mathcal{B}_w w_k(t), \\ y_k(t) =& \mathcal{C}\mathcal{X}_k(t), \end{aligned} \tag{17}$$

where $\mathcal{X}_k(t) = [x_k^T(t) \quad \hat{X}_k^T(t) \quad \sum e_k^{s,T}(t-1)]^T$, $\mathcal{A}_k(t)$ and $\mathcal{A}_{h,k}(t)$ are $\mathcal{A}(t)$ and $\mathcal{A}_h(t)$ with the subscript k added, respectively, and $\mathcal{B}_k(t) = \mathcal{B}+\mathcal{E}\Delta_k(t)F_bK_{pi}$, $\mathcal{B} = [(BK_{pi})^T \quad (\hat{B}K_{pi})^T \quad \mathrm{I}]^T$.

The set-point ILC law applied is

$$y_k^s(t) = y_{k-1}^s(t) + \Gamma e_{k-1}(t+1), \tag{18}$$

where Γ is the learning gain, $e_{k-1}(t+1)$, denotes the one-step ahead tracking error from the previous trial (at the end of a trial, all information generated is, at the cost of storage, available for use in updating the control input for the subsequent trial), and it follows that $\delta\mathcal{X}_k(t) = 0$ for any $t \leq 0$. Moreover, calculating the increments of (2) and (17) in the along the trial direction yields

$$\begin{aligned} \delta\mathcal{X}_k(t+1) =& \mathcal{A}_k(t-1)\delta\mathcal{X}_k(t) + \mathcal{A}_{h,k}(t-1)\delta\mathcal{X}_k(t-h) \\ &+ \mathcal{B}_k(t-1)\Gamma e_{k-1}(t) + \varpi_k(t), \end{aligned} \tag{19}$$

where

$$\varpi_k(t) = \delta\mathcal{A}_k(t)\mathcal{X}_{k-1}(t-1)+\delta\mathcal{A}_{h,k}(t)\mathcal{X}_{k-1}(t-1-h)+\delta\mathcal{B}_k(t)y_{k-1}^s(t-1)+\mathcal{B}_w\delta w_k(t).$$

Also, using (19) it follows that

$$\begin{aligned} e_k(t) =& e_{k-1}(t) - \mathcal{C}\delta\mathcal{X}_k(t+1) \\ =& [\mathrm{I} - \mathcal{C}\mathcal{B}_k(t-1)\Gamma]e_{k-1}(t) + \Theta_k(t), \end{aligned} \tag{20}$$

where $\Theta_k(t) = -\mathcal{C}\mathcal{A}_k(t-1)\delta\mathcal{X}_k(t) - \mathcal{C}\mathcal{A}_{h,k}(t-1)\delta\mathcal{X}_k(t-h) - \mathcal{C}\varpi_k(t)$.

3.3 ILC Convergence analysis

The choice of Γ to implement the set-point ILC law is an outcome of the following ILC robust convergence result.

Theorem 3.2 *Consider the system described in* (17) *under the set-point ILC law in* (18)*. Then the condition for bounded tracking* (3) *and the boundedness conditions of* (4) *are guaranteed under Assumption 1 if there exists a scalar gain* Γ *such that the following two conditions are both satisfied with* $\lambda \in (0, 1]$

$$\|\mathrm{I} - \Gamma CB_{k-1}(t)K_{pi}\| < \lambda, \tag{21}$$

$$\|\mathrm{I} - CB_{k-1}(t)K_{pi}\Gamma\| < \lambda. \tag{22}$$

Proof 2 *Rewriting* (18) *gives*

$$\begin{aligned} y_k^s(t) =& y_{k-1}^s(t) + \Gamma[y_d(t+1) - \mathcal{C}\mathcal{X}_{k-1}(t+1)] \\ =& [\mathrm{I} - \Gamma\mathcal{C}\mathcal{B}_{k-1}(t)]y_{k-1}^s(t) + \Phi_k(t) + \phi_k^s(t), \end{aligned} \tag{23}$$

where

$$\begin{aligned} \phi_k^s(t) =& \Gamma y_d(t+1) - \Gamma\mathcal{C}\mathcal{B}_w w_{k-1}(t), \\ \Phi_k(t) =& -\Gamma\mathcal{C}\mathcal{A}_{k-1}(t)\mathcal{X}_{k-1}(t) - \Gamma\mathcal{C}\mathcal{A}_{h,k-1}(t)\mathcal{X}_{k-1}(t-h). \end{aligned}$$

Also, $\|\phi_k^s(t)\| \leq \|\Gamma\|(\beta_r + \|C\|\|B_w\|\beta_w)$ *for any* $k \in \mathbb{Z}_+$ *and* $t \in \mathbb{Z}_N$*. By selecting finite* L*,* K_x*,* K_p *and* K_i *in (10), it follows that* $\mathcal{A}_k(t)$*,* $\mathcal{A}_{h,k}(t)$ *and* $\mathcal{B}_k(t)$ *are bounded for any* $k \in \mathbb{Z}_+$ *and* $t \in \mathbb{Z}_N$ *under Assumption 1, with bounds denoted by* $\beta_{\mathcal{A}}$*,* $\beta_{\mathcal{A}_h}$ *and* $\beta_{\mathcal{B}}$*, respectively.*

The following analysis uses mathematical induction to verify the boundedness conditions in (4) *for any* $k \in \mathbb{Z}_+$ *and* $t \in \mathbb{Z}_N$*.*

Step (i): *For* $t = 0$*,* $\|\Phi_k(0)\| \leq \|\Gamma\|\|C\|(\beta_{\mathcal{A}} + \beta_{\mathcal{A}_h})\beta_{\mathcal{X}}(0)$ *for any* $k \in \mathbb{Z}_+$*, where* $\beta_{\mathcal{X}}(0) = \|x_0\|$*. Therefore, by the result of Lemma 2 for* (23) *at* $t = 0$*, it follows that* $y_k^s(0)$ *is bounded, with bound denoted by* $\sup_{k\in\mathbb{Z}_+}\|y_k^s(0)\| \leq \beta_s(0) < \infty$*.*

Step (ii): *For any given* $t \in \mathbb{Z}_{N-1}$*, assume that* $\sup_{k\in\mathbb{Z}_+}\|\mathcal{X}_k(t)\| \leq \beta_{\mathcal{X}}(t) < \infty$ *and* $\sup_{k\in\mathbb{Z}_+}\|y_k^s(t)\| \leq \beta_s(t) < \infty$*, respectively. Then for* $t+1$*, it is proved that* $\sup_{k\in\mathbb{Z}_+}\|\mathcal{X}_k(t+1)\| \leq \beta_{\mathcal{X}}(t+1) < \infty$ *and* $\sup_{k\in\mathbb{Z}_+}\|y_k^s(t+1)\| \leq \beta_s(t+1) < \infty$*.*

Based on this last boundedness hypothesis on $\mathcal{X}_k(t)$ *and* $y_k^s(t)$*, it follows from* (17) *that*

$$\begin{aligned} \|\mathcal{X}_k(t+1)\| \leq& \|\mathcal{A}_k(t)\|\|\mathcal{X}_k(t)\| + \|\mathcal{A}_{h,k}(t)\|\|\mathcal{X}_k(t-h)\| \\ &+ \|\mathcal{B}_k(t)\|\|y_k^s(t)\| + \|\mathcal{B}_w\|\|w_k(t)\| \\ \leq& \beta_{\mathcal{A}}\beta_{\mathcal{X}}(t) + \beta_{\mathcal{A}_h}\beta_{\mathcal{X}}(t-h) + \beta_{\mathcal{B}}\beta_s(t) + \|B_w\|\beta_w \\ \triangleq& \beta_{\mathcal{X}}(t+1),\ \forall k \in \mathbb{Z}_+, \end{aligned} \tag{24}$$

and hence

$$\|\Phi_k(t+1)\| \leq \|\Gamma\|\|C\|[\beta_{\mathcal{A}}\beta_{\mathcal{X}}(t+1) + \beta_{\mathcal{A}_h}\beta_{\mathcal{X}}(t+1-h)], \forall k \in \mathbb{Z}_+. \tag{25}$$

Applying Lemma 2 to (23) *at sample* $t+1$ *verifies that* $\sup_{k\in\mathbb{Z}_+}\|y_k^s(t+1)\| \leq \beta_s(t+1)$*. This fact, together with* (24)*, implies that the hypothesis made in this step holds, i.e.,*

$$\sup_{k\in\mathbb{Z}_+}\max_{t\in\mathbb{Z}_{N-1}}\|y_k^s(t)\| \leq \beta_s,\ \sup_{k\in\mathbb{Z}_+}\max_{t\in\mathbb{Z}_N}\|\mathcal{X}_k(t)\| \leq \beta_{\mathcal{X}},$$

with $\beta_s = \max_{t\in\mathbb{Z}_{N-1}} \beta_s(t)$ *and* $\beta_{\mathcal{X}} = \max_{t\in\mathbb{Z}_N} \beta_{\mathcal{X}}(t)$. *Given the relationships between* $y_k^s(t)$ *and* $u_k(t)$ *given in* (9) *and* (10)*, between* $\mathcal{X}_k(t)$ *and* $x_k(t)$ *in* (17)*, the boundedness conditions of* $u_k(t)$ *and* $x_k(t)$ *are satisfied by* (21)*. Further, it follows from* (20) *that*

$$\|\Theta_k(t)\| \leq 2\|C\|\beta_{\mathcal{A}}\beta_{\mathcal{X}} + 2\|C\|\beta_{\mathcal{A}_h}\beta_{\mathcal{X}} + 2\|C\|[\beta_{\mathcal{A}}\beta_{\mathcal{X}} + \beta_{\mathcal{A}_h}\beta_{\mathcal{X}} + \beta_{\mathcal{B}}\beta_s + \|B_w\|\beta_w] < \infty.$$

Hence, the bounded tracking goal in (3) *can be ensured by applying Lemma 2 to the error dynamics in* (20) *based on* (22)*.*

The sufficient conditions in the last result are delay-independent, and are difficult to verify. However, using (19) and (20), the controlled ILC dynamics can be written in the form

$$\begin{aligned} \delta\mathcal{X}_k(t+1) =& \mathbb{A}\delta\mathcal{X}_k(t) + \mathbb{A}_h\delta\mathcal{X}_k(t-h) + \mathbb{B}e_{k-1}(t) + \varpi_k(t), \\ e_k(t) =& \mathbb{C}\delta\mathcal{X}_k(t) + \mathbb{C}_h\delta\mathcal{X}_k(t-h) + \mathbb{D}e_{k-1}(t) - \mathcal{C}\varpi_k(t), \end{aligned} \tag{26}$$

where

$$\begin{aligned} \mathbb{A} =& \mathcal{A} + \mathcal{E}\Delta_k(t-1)\mathcal{F}_1,\ \mathbb{A}_h = \mathcal{A}_h + \mathcal{E}\Delta_k(t-1)\mathcal{F}_h,\ \mathbb{C}_h = -\mathcal{C}\mathbb{A}_h, \\ \mathbb{B} =& \mathcal{B}\Gamma + \mathcal{E}\Delta_k(t-1)\mathcal{F}_b,\ \mathcal{F}_b = F_bK_{pi}\Gamma, \mathbb{C} = -\mathcal{C}\mathbb{A},\ \mathbb{D} = \mathrm{I} - \mathcal{C}\mathbb{B}. \end{aligned}$$

An ILC design is required to enforce trial-to-trial error convergence (in k) and ensure acceptable dynamics during the trials (in t). Hence, information propagates in two independent directions. In which context, the state-space model (26) is that for a discrete linear repetitive process and hence as shown next the problem of controller synthesis can be transformed to an equivalent repetitive process stability problem.

Repetitive processes make repeated sweeps (or trials in the terminology used in this paper) through a set of dynamics defined over a finite duration, known as the trial length. Once a trial is complete, the dynamics reset to the starting position, or there is a stoppage time between the end of one trial and the start of the next. Also, the output produced during a trial directly affects the dynamics of the subsequent trial, hence the possibility of oscillations that increase in amplitude from trial to trial, which cannot be controlled by standard action. A stability theory for these processes has been developed to prevent this unacceptable feature from arising.

The stability theory requires that a bounded initial trial output generates a bounded sequence of trial outputs, either over the finite trial length or uniformly, i.e., for all possible finite trial lengths, where boundedness is defined in terms of the norm on the underlying signal space [9]. Convergence in k is feasible even for unstable linear systems. Hence, the stronger property, known as stability along the trial, is generally required.

In common with standard linear systems theory, one approach to control law design is to use a suitably constructed Lyapunov function, which should be constructed from the sum of terms in the trial-to-trial propagation (e_k in (26)) and the along the trial dynamics ($\delta\mathcal{X}_k(t)$ in (26)), respectively, but the two equations in (26)) are coupled and hence the gradient of the Lyapunov function can only be found provided the solutions to these equations are available, which is a very stringent requirement and instead a vector Lyapunov function must be used and the gradient replaced by the divergence, see [8] for the required background.

Let $V(k,t)$ denote the vector Lyapunov function and take this to be the sum of $V_{hor}(k,t)$ and $V_{ver}(k,t)$ where

$$\begin{aligned} V_{hor}(t,k) =& \delta\mathcal{X}_k^T(t)P\delta\mathcal{X}_k(t) + \sum_{i=t-h}^{t-1}\delta\mathcal{X}_k^T(i)Q\delta\mathcal{X}_k(i) + \bar{h}\sum_{j=-\bar{h}}^{-1}\sum_{i=t+j}^{t-1}\sigma_k^T(i)R\sigma_k(i), \\ V_{ver}(k,t) =& e_{k-1}^T(t)Se_{k-1}(t), \end{aligned} \tag{27}$$

where $\sigma_k(i) = \delta\mathcal{X}_k(i+1) - \delta\mathcal{X}_k(i)$, and $P \succ 0$, $R \succ 0$, $Q \succ 0$, $S \succ 0$ and $h \in \mathbb{Z}_{\bar{h}}$.

Theorem 3.3 *Given an $\mathcal{H}_\infty$ performance γ_{ilc} and a user-specified learning gain Γ, the linear repetitive process representation of the ILC dynamics described in* (26) *is robustly stable along the trial for any state delay h satisfying $h \in \mathbb{Z}_{\bar{h}}$, where $\bar{h}$ is a known upper bound, if there exist matrices $W_i \succ 0, i = 1, \cdots, 5$, and a scalar $\varepsilon > 0$, such that the following LMI is feasible*

$$\begin{bmatrix} \theta_{11} & \theta_{12} & \theta_{13} & \theta_{14} & \theta_{15} & \theta_{16} & \mathrm{I} & 0 \\ (*) & \theta_{22} & \theta_{23} & \theta_{24} & \theta_{25} & \theta_{26} & \bar{h}\mathrm{I} & 0 \\ (*) & (*) & \theta_{33} & \theta_{34} & \theta_{35} & \theta_{36} & -\mathcal{C} & 0 \\ (*) & (*) & (*) & \theta_{44} & W_2 & 0 & 0 & \theta_{48} \\ (*) & (*) & (*) & (*) & \theta_{55} & 0 & 0 & \theta_{58} \\ (*) & (*) & (*) & (*) & (*) & -W_3 & 0 & \theta_{68} \\ (*) & (*) & (*) & (*) & (*) & (*) & -\gamma_{ilc}^2\mathrm{I} & 0 \\ (*) & (*) & (*) & (*) & (*) & (*) & (*) & -\varepsilon\mathrm{I} \end{bmatrix} \prec 0, \tag{28}$$

where $\theta_{11} = -W_1 + \varepsilon\mathcal{E}\mathcal{E}^T$, $\theta_{12} = \varepsilon\bar{h}\mathcal{E}\mathcal{E}^T$, $\theta_{13} = -\varepsilon\mathcal{E}\mathcal{E}^T\mathcal{C}^T$, $\theta_{14} = \mathcal{A}W_2$, $\theta_{15} = \mathcal{A}_hW_2$, $\theta_{16} = \mathcal{B}\Gamma W_3$, $\theta_{22} = -W_2 + \varepsilon\bar{h}^2\mathcal{E}\mathcal{E}^T$, $\theta_{23} = -\varepsilon\bar{h}\mathcal{E}\mathcal{E}^T\mathcal{C}^T$, $\theta_{24} = \bar{h}\varphi_{14} - \bar{h}W_2$, $\theta_{25} = \bar{h}\varphi_{15}$, $\theta_{26} = \bar{h}\varphi_{16}$, $\theta_{33} = -W_3 - \varepsilon\mathcal{C}\mathcal{E}\mathcal{E}^T\mathcal{C}^T$, $\theta_{34} = -\mathcal{C}\varphi_{14}$, $\theta_{35} = -\mathcal{C}\varphi_{15}$, $\theta_{36} = W_3 - \mathcal{C}\varphi_{16}$, $\theta_{44} = -W_4 + W_5 - W_2$, $\theta_{48} = (\mathcal{F}_1W_2)^T$, $\theta_{55} = -W_5 - W_2$, $\theta_{58} = (\mathcal{F}_hW_2)^T$, $\theta_{68} = (\mathcal{F}_bW_3)^T$.

Proof 3 *The divergence operator of $V(k,t)$ in this case is*

$$\Delta V(k,t) = \Delta V_{hor}(k,t) + \Delta V_{ver}(k,t), \tag{29}$$

where $\Delta V_{hor}(k,t) = V_{hor}(k,t+1) - V_{hor}(k,t)$ *and* $\Delta V_{ver}(k,t) = V_{ver}(k+1,t) - V_{ver}(k,t)$. *Moreover, it follows that*

$$\begin{aligned}\Delta V(k,t) \leq & \delta\mathcal{X}_k^T(t+1)P\delta\mathcal{X}_k(t+1) - \delta\mathcal{X}_k^T(t)P\delta\mathcal{X}_k(t) + \delta\mathcal{X}_k^T(t)Q\delta\mathcal{X}_k(t) \\ & - \delta\mathcal{X}_k^T(t-h)Q\delta\mathcal{X}_k(t-h) + \sigma_k^T(t)\bar{h}^2R\sigma_k(t) \\ & - [\delta\mathcal{X}_k(t) - \delta\mathcal{X}_k(t-h)]^T R[\delta\mathcal{X}_k(t) - \delta\mathcal{X}_k(t-h)] \\ & + e_k^T(t)Se_k(t) - e_{k-1}^T(t)Se_{k-1}(t) \\ = & \phi_k^T(t)\Psi\phi_k(t),\end{aligned} \tag{30}$$

where

$\phi_k(t) = [\delta\mathcal{X}_k^T(t)\ \delta\mathcal{X}_k^T(t-h)\ e_{k-1}^T(t)]^T$, $\Psi = \Psi_1^T P\Psi_1 + \bar{h}^2\Psi_2^T R\Psi_2 + \Psi_3^T S\Psi_3 + \Xi$,

$\Psi_1 = [\mathbb{A} \quad \mathbb{A}_h \quad \mathbb{B}]$, $\Psi_2 = [\mathbb{A} - \mathrm{I} \quad \mathbb{A}_h \quad \mathbb{B}]$, $\Psi_3 = [\mathbb{C} \quad \mathbb{C}_h \quad \mathbb{D}]$,

and

$$\Xi = \begin{bmatrix} -P+Q-R & R & 0 \\ (*) & -Q-R & 0 \\ (*) & (*) & -S \end{bmatrix}.$$

Introduce the cost function

$$J = \sum_{t=0}^{N}\sum_{k=1}^{\infty}[e_k^T(t)e_k(t) - \gamma_{ilc}^2\varpi_k^T(t)\varpi_k(t)]. \tag{31}$$

Then, using the boundary conditions (2), *there exist* $\delta\mathcal{X}_k(t) = 0$ *for any* $t \leq 0$ *and* $\forall k \in \mathbb{Z}_+$, *and* $\delta\mathcal{X}_0(t) = 0$ *for* $t \in \mathbb{Z}_N$. *Hence, it follows that*

$$\begin{aligned}J < & \sum_{t=0}^{N}\sum_{k=1}^{\infty}[e_k^T(t)e_k(t) - \gamma_{ilc}^2\varpi_k^T(t)\varpi_k(t) + \Delta V(k,t)] \\ < & \sum_{t=0}^{N}\sum_{k=1}^{\infty}\xi_k^T(t)\hat{\Psi}\xi_k(t),\end{aligned} \tag{32}$$

where $\hat{\Psi} = \hat{\Psi}_1^T P\hat{\Psi}_1 + \bar{h}^2\hat{\Psi}_2^T R\hat{\Psi}_2 + \hat{\Psi}_3^T(S+\mathrm{I})\hat{\Psi}_3 + \hat{\Xi}$, $\xi_k(t) = [\phi_k^T(t) \quad \varpi_k^T(t)]^T$, $\hat{\Psi}_1 = [\Psi_1 \quad \mathrm{I}]$, $\hat{\Psi}_2 = [\Psi_2 \quad \mathrm{I}]$, $\hat{\Psi}_3 = [\Psi_3 \quad -\mathcal{C}]$, $\hat{\Xi} = \mathrm{diag}\{\Xi, -\gamma_{ilc}^2\mathrm{I}\}$. *Finally, by applying Lemma 1 and similar steps as in the proof of Theorem 1, the LMI of (28) is obtained.*

4 Case Study

4.1 Example 1

In order to verify the effectiveness of the proposed indirect-type ILC scheme, the injection molding process as studied by [1] is used. The injection molding

process mainly includes four stages: filling, packing, cooling and demolding. During the packing stage, the nozzle pressure is a key process variable that needs to be controlled. In order to ensure the quality and consistency of the product in the batch direction, the pressure should track the expected output trajectory. However, due to the adverse effects of the production environment and operation changes in various batches, this makes the packing stage a time-varying dynamic process, such as the uneven supply of materials, the nonlinear dynamic characteristics of the hydraulic control valve, the pressure of the mold cavity, the temperature change, etc. Among them, the impact caused by the pressure of the cavity can be regarded as a load disturbance with non-repetitive characteristics. Based on the open-loop test and analysis, the system matrices of injection velocity relative to valve opening has been identified as

$$\begin{aligned} A &= \begin{bmatrix} 1.607 & 1 \\ -0.6086 & 0 \end{bmatrix}, A_h = \begin{bmatrix} -0.202 & 0 \\ 0.196 & 0 \end{bmatrix}, B = \begin{bmatrix} 1.2390 \\ -0.9282 \end{bmatrix}, \\ \Delta A_k(t) &= \begin{bmatrix} 0.08\delta_{1,k}(t) & 0 \\ 0.08\delta_{2,k}(t) & 0 \end{bmatrix}, \Delta A_{h,k}(t) = \begin{bmatrix} 0.01\delta_{3,k}(t) & 0 \\ 0.01\delta_{4,k}(t) & 0 \end{bmatrix}, \\ \Delta B_k(t) &= \begin{bmatrix} 0.1\delta_{5,k}(t) \\ 0.14\delta_{6,k}(t) \end{bmatrix}, B_w = \begin{bmatrix} 1 \\ 0 \end{bmatrix}, C = \begin{bmatrix} 1 & 0 \end{bmatrix}. \end{aligned}$$

where $x_k(0) = x_0 + \partial_k(t)$, $x_0 = [0 \quad 0]^T$, $\partial_k(t) = [\delta_{7,k}^T(t) \quad \delta_{8,k}^T(t)]^T$, $w_k(t) = \sin(0.1t) + \delta_{9,k}(t)$, and $\delta_{i,k}(t), i = 1, 2, \cdots, 9$, are non-repetitive parameters that vary randomly within $[-0.1, 0.1]$. The time delay range is assumed to be $h \in \mathbb{Z}_{\bar{h}}$ and $\bar{h} = 3$, where $h = 3$ is used in the simulation results below. The reference trajectory is

$$y_d(t) = \begin{cases} 200, & 0 \le t \le 100; \\ 200 + 5(t - 100), & 100 < t \le 120; \\ 300, & 120 < t \le N = 200. \end{cases}$$

Given that this signal is not continuous, the initial part of it is smoothed by a user-specified prefilter $G_f(z) = \frac{z^{-1}+z^{-2}}{3-z^{-1}}$ (where z is the forward shift) as used in [4]. Note that this last step is application-specific, and the design can be applied in applications where such prefiltering is not required.

Criteria are required to assess the performance of the controlled dynamics. Standard linear systems measures can be used on any trial (t). In the case of the trial-to-trial error convergence, a commonly used measure is the root mean square error (RMS_k) plotted against k, where on this trial

$$RMS_k = \sqrt{\frac{1}{N}\sum_{i=1}^{N} e_k^2(i)}.$$

By solving the minimization problem in (16), the optimal $\mathcal{H}_\infty$ control performance is computed as $\gamma_{pi} = 0.0049$. To avoid over-aggressive control actions, a feasible solution of performance index $\gamma_{pi} = 0.8436$ is taken to solve the LMI in (12), and the gains of the inner loop feedback controller and observer are obtained as

$$\begin{aligned} K_x =&[-0.049 \quad -0.0749 \quad -0.0375 \quad 0.0616],\ K_p = 0.3627,\ K_i = 0.1557, \\ L =&[0.6127 \quad -0.5228 \quad -0.001 \quad 0.0007]^T. \end{aligned}$$

Accordingly, $\Gamma = 0.9572$ is used in the set-point ILC law, which satisfies both the conditions in Theorems 3.2 and 3.3.

For comparison, two alternative ILC laws are considered, the first from [16], where

$$\begin{aligned} u_k(t) &= 0.0412 e_k^s(t) + 0.00017 \sum e_k^s(t), \\ y_k^s(t) &= y_{k-1}^s(t) - 0.0044\delta \sum e_k^s(t) + 1.6 e_{k-1}(t+1). \end{aligned}$$

and the second from [17] where

$$u_k(t) = u_{k-1}(t) - 0.6525\delta y_k(t+1) + 0.4706 e_{k-1}(t) + 0.4779[e_{k-1}(t+1) - e_{k-1}(t)].$$

A comparison is also made with

$$u_k(t) = u_{k-1}(t) + 0.0572 e_{k-1}(t+1)$$

(phase-lead ILC). Next the performance of the design is examined, starting with the nominal dynamics.

Case 1.1 (nominal system). Assume that there are no uncertainties and disturbances in the system. The tracking results are shown in Fig. 2, and the resulting RMS errors are shown in Fig. 3. It is seen that no steady-state error tracking is achieved in the first trial, and the perfect tracking is realized after five trials by the new indirect-type ILC scheme, while the ILC-based PI control method in [16] requires more than 20 batches. Comparing the direct-type ILC methods in [17] and open-loop P-type ILC, the tracking performance is markedly improved due to the PI feedback control in the inner loop, especially in the initial trial.

Case 1.2 (non-repetitive uncertainties and disturbances). In the presence of time- and batch-varying uncertainties and disturbances, the tracking results are shown in Fig. 4 and the result for the RMS error against the trial number are plotted in Fig 5. Compared with the ILC-based PI control in [16] and the direct-type ILC method in [17], the set-point tracking and disturbance rejection performance is markedly enhanced due to the

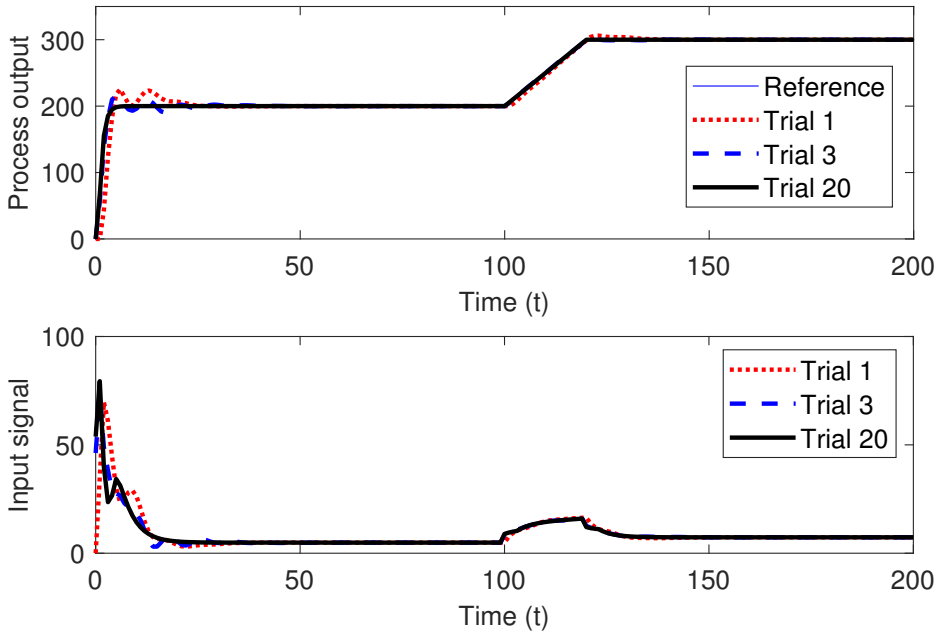

Figure 2: Results for Case 1.1.

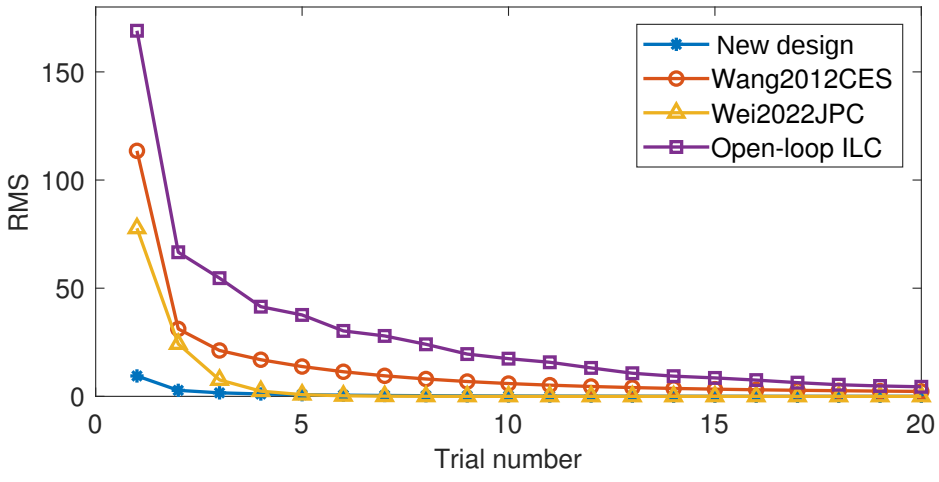

Figure 3: The RMS performance index for Case 1.1.

estimation and feed-forward compensation of the total disturbance. It can be seen that the bounded tracking goal in (3) and (4) is achieved by the new design, which illustrates the validity and superiority of the indirect-type ILC design.

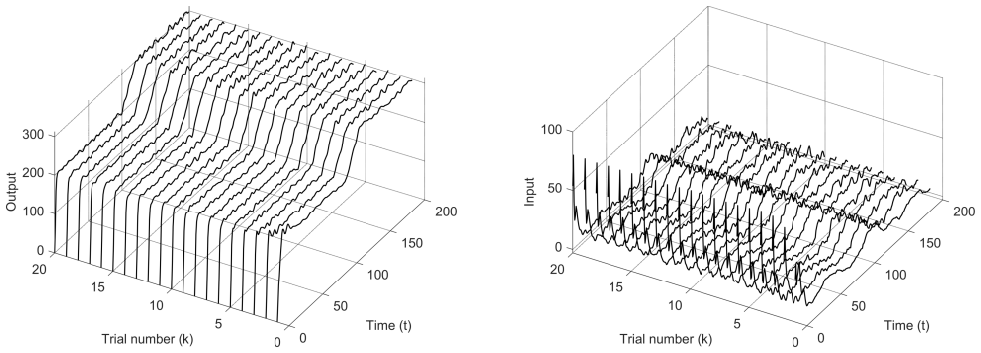

Figure 4: Results for Case 1.2.

4.2 Example 2

To showcase the feasibility and effectiveness of the proposed method, a two-stage chemical reactor with delayed recycle streams is considered. Detailed information on this setup can be found in paper [13], where the state-space model of this continuous-time system is

$$A_c = \begin{bmatrix} -2.5 & 0 \\ 1 & -2.5 \end{bmatrix}, B_c = \begin{bmatrix} 1 & 0 \\ 0 & 1 \end{bmatrix}, C_c = \begin{bmatrix} 1 & 0 \\ 0 & 1 \end{bmatrix}.$$

The sampling time is set to $T_s = 0.1s$ and the discretised system matrix is obtained using a zero-order holder

$$A = \begin{bmatrix} 0.7788 & 0 \\ 0.0779 & 0.7788 \end{bmatrix}, B = \begin{bmatrix} 0.0885 & 0 \\ 0.0042 & 0.0885 \end{bmatrix}, C = \begin{bmatrix} 1 & 0 \\ 0 & 1 \end{bmatrix},$$

and the uncertainties are specified by

$$A_h = \begin{bmatrix} 0 & 0.04 \\ 0 & 0 \end{bmatrix}, B_w = \begin{bmatrix} 1 & 0 \\ 0 & 1 \end{bmatrix}, E = \begin{bmatrix} 1 & 0 \\ 0.5 & 1 \end{bmatrix},$$
$$F_a = \begin{bmatrix} 0.04 & 0 \\ 0 & 0.05 \end{bmatrix}, F_h = \begin{bmatrix} 0 & 0.05 \\ 0 & 0 \end{bmatrix}, F_b = \begin{bmatrix} 0.01 & 0 \\ 0 & 0.01 \end{bmatrix}.$$

The time delay range is assumed to be $h \in \mathbb{Z}_{\bar{h}}$ and $\bar{h} = 3$, where $h = 3$ is used in the simulation results below. Similarly, the convergence of the

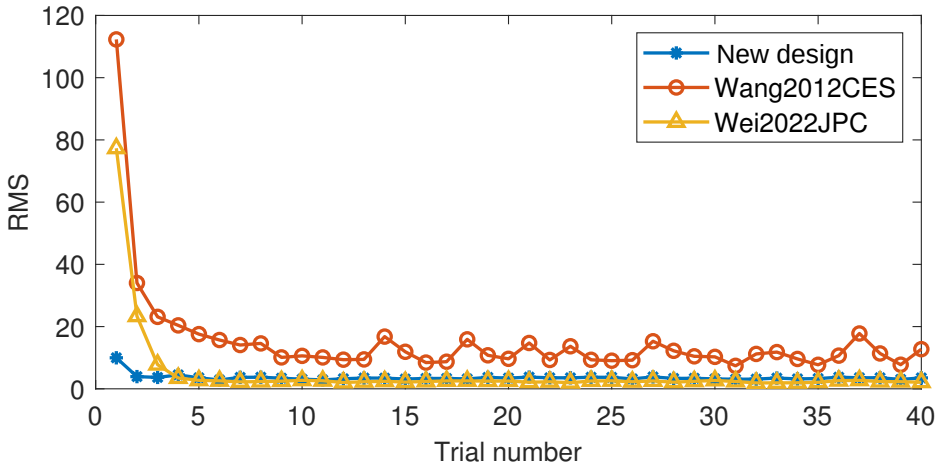

Figure 5: The RMS performance index for Case 1.2.

tracking error $e_{ki}, i = 1, 2$ is measured using the RMS_k. The initial state $x_k(0)$ is assumed to be zero $\forall k \in \mathbb{Z}_+$ and the reference trajectories are

$$y_{d1}(t) = \begin{cases} \frac{1}{20}t, & 0 \le t \le 40; \\ 2 + \frac{1}{120}(t-40), & 40 < t \le 100; \\ 2.5 + \frac{1}{300}(t-100), & 100 < t \le 250; \\ 3, & 250 < t \le N = 300. \end{cases}$$

$$y_{d2}(t) = \begin{cases} \frac{1}{120}t, & 0 \le t \le 60; \\ 0.5 + \frac{1}{60}(t-60), & 60 < t \le 120; \\ 1.5, & 120 < t \le 150; \\ 1.5 + \frac{1}{100}(t-150), & 150 < t \le 250; \\ 2.5, & 250 < t \le N = 300. \end{cases}$$

A feasible solution of performance index $\gamma_{pi} = 0.8965$ is taken to solve the LMI in (12), and the gains of the inner loop feedback controller and observer are obtained as

$$K_x = \begin{bmatrix} 1.0962 & 0.0855 & -1.0513 & -0.0741 \\ -0.0874 & 1.1064 & 0.0751 & -1.0562 \end{bmatrix},$$

$$K_p = \begin{bmatrix} 3.0692 & -0.3641 \\ 0.3705 & 3.0254 \end{bmatrix}, K_i = \begin{bmatrix} 0.2999 & 9.0391e^{-5} \\ -1.0146e^{-4} & 0.2999 \end{bmatrix},$$

$$L = \begin{bmatrix} 0.8704 & 0.0362 & 0.3472 & -4.2363e^{-5} \\ -0.0369 & 0.8656 & -5.4959e^{-4} & 0.3470 \end{bmatrix}^T.$$

Accordingly, $\Gamma = \text{diag}\{0.51, 0.51\}$ is used in the set-point ILC law, which satisfies both the conditions in Theorems 3.2 and 3.3. Similarly, next two possible cases are considered.

Case 2.1 (nominal system). Assume that there are no uncertainties and disturbances in the system. The tracking results are shown in Figs. 6 and 7, and the resulting RMS errors are shown in Fig. 8. It is seen that steady-state tracking is achieved in the first trial, and the perfect tracking is realized after ten trials by the new indirect-type ILC scheme.

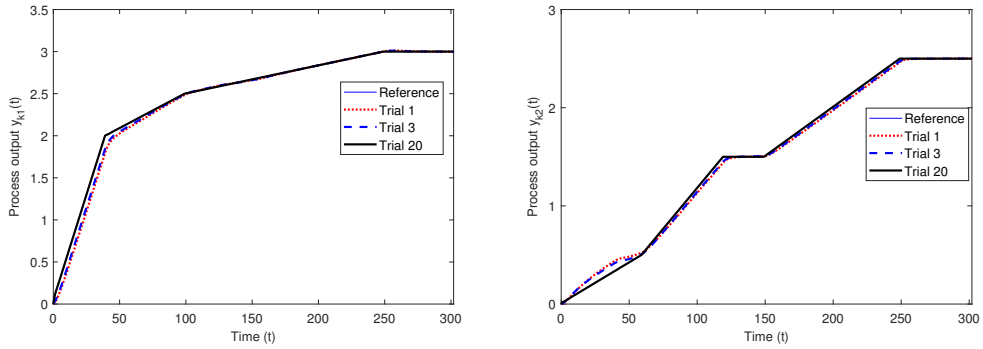

Figure 6: The process outputs for Case 2.1.

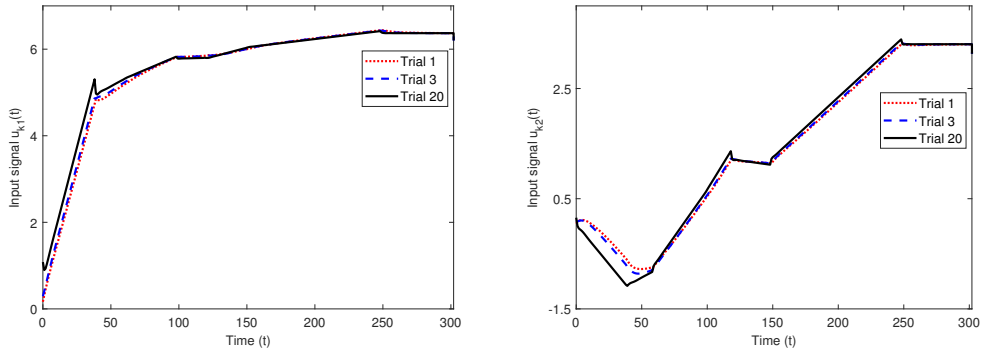

Figure 7: The control inputs for Case 2.1.

Case 2.2 (non-repetitive uncertainties and disturbances). In the presence of time- and batch-varying uncertainties and disturbances, assume that $\Delta_k(t) = \text{diag}\{\delta_{k1}(t), \delta_{k2}(t)\}$ and $w_k(t) = [\delta_{k3}(t), \delta_{k4}(t)]^T$, where $\delta_{ki}, i = 1, \cdots, 4$ are random variables within $[-0.05, 0.05]$. The tracking results are shown in Figs. 9 and 10, and the resulting RMS errors are shown in Fig. 11. Although the designed control scheme cannot completely eliminate the effects of non-repetitive uncertainties and disturbances, the bounded tracking objective in (3) and (4) is achieved, which illustrates the effectiveness of the indirect-type ILC design.

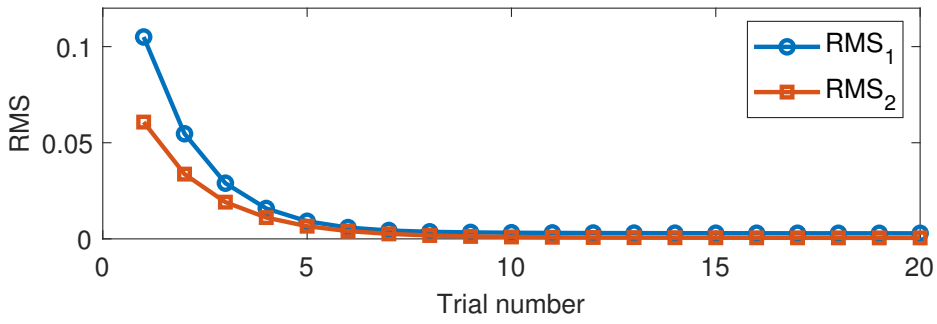

Figure 8: The RMS performance index for Case 2.1.

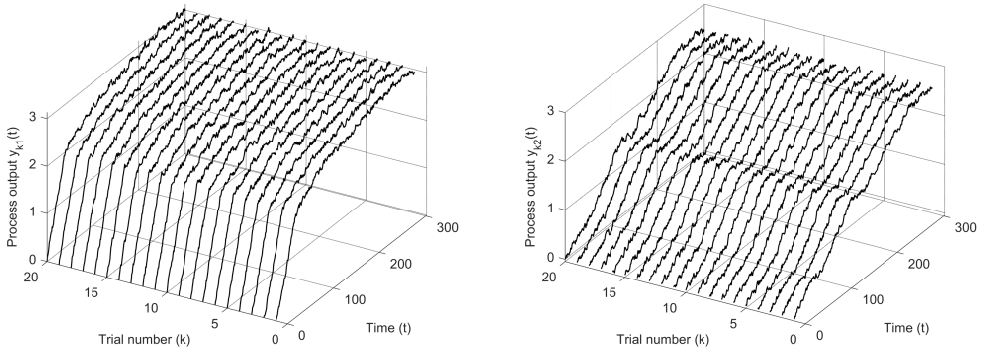

Figure 9: The process outputs for Case 2.2.

5 Conclusion

For batch processes with state delay and time- and batch-varying uncertainties, a robust indirect-type set-point ILC scheme has been developed, which consists of two loops, inner and outer, respectively, that can be separately designed. In the inner loop, current state feedback GESO is augmented by PI control acting on the error. A P-type learning law updates the set-point command in the outer loop. Moreover, both delay-independent and delay-dependent sufficient conditions are derived to ensure error convergence and robust stability along the trial by using the mathematical induction and Lyapunov-Krasovskii analysis methods, respectively. Compared with the previously developed direct-type and indirect-type ILC methods, two illustrative examples have been used to demonstrate the validity and advantages of the new design.

Acknowledgement 1 *This work was partially supported by the National Natural Science Foundation of China (Nos. 61773181, 61203092, 61903060), 111 Project (B23008), the Fundamental Research Funds for the Central Universities (No. JUSRP51733B), and the National Science Centre in Poland,*

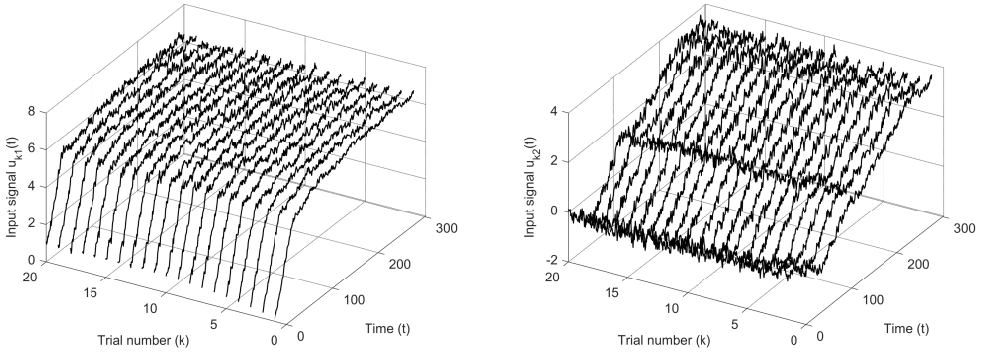

Figure 10: The control inputs for Case 2.2.

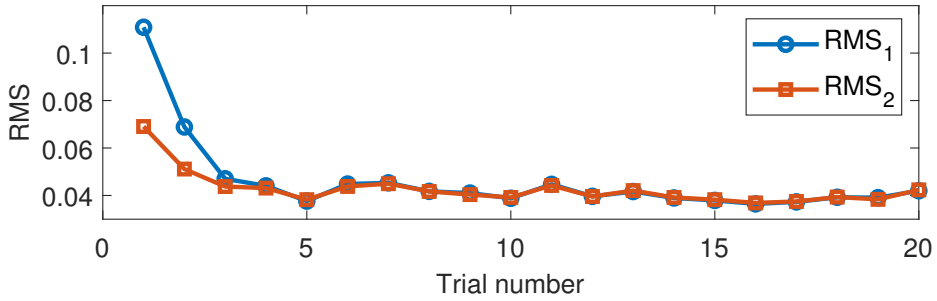

Figure 11: The RMS performance index for Case 2.2.

grant No. 2023/48/Q/ST7/00205.

References

[1] S. L. Hao, T. Liu, and E. Rogers. Extended state observer based indirect-type ILC for single-input single-output batch processes with time-and batch-varying uncertainties. *Automatica*, 112:108673, 2020.

[2] Y. Hui, R.-H. Chi, B. Huang, and Z.-S. Hou. Extended state observer-based data-driven iterative learning control for permanent magnet linear motor with initial shifts and disturbances. *IEEE Transactions on Systems, Man, and Cybernetics: Systems*, 51(3):1881–1891, 2019.

[3] J. X. Liu, T. Liu, J. H. Chen, H. Yue, F. K. Zhang, and F. R. Sun. Data-driven modeling of product crystal size distribution and optimal input design for batch cooling crystallization processes. *Journal of Process Control*, 96:1–14, 2020.

[4] T. Liu and F. R. Gao. Robust two-dimensional iterative learning control for batch processes with state delay and time-varying uncertainties. *Chemical Engineering Science*, 65(23):6134–6144, 2010.

[5] T. Liu, X. Z. Wang, and J. Chen. Robust PID based indirect-type iterative learning control for batch processes with time-varying uncertainties. *Journal of Process Control*, 24(12):95–106, 2014.

[6] T. Liu, S.-L. Hao, Y.-Q. Wang, and J. Nal. Predictive state observer based set-point learning control for batch manufacturing processes with delay response. *IEEE Transactions on Industrial Electronics*, 71(1):788–797, 2023.

[7] D.-Y. Meng and K. L. Moore. Robust iterative learning control for non-repetitive uncertain systems. *IEEE Transactions on Automatic Control*, 62(2):907–913, 2017.

[8] P. Pakshin, J. Emelianova, M. Emelianov, K. Gałkowski, and E. Rogers. Dissipivity and stabilization of nonlinear repetitive processes. *Systems and Control Letters*, 91:14–20, 2016.

[9] E. Rogers, K. Gałkowski, and D. H. Owens. *Control Systems Theory and Applications for Linear Repetitive Processes*, volume 349 of *Lecture Notes in Control and Information Sciences*. Springer-Verlag, Berlin, Germany, 2007.

[10] E. Rogers, B. Chu, C. Freeman, and P. Lewin. *Iterative Learning Control Algorithms and Experimental Benchmarking*. Wiley, 2023. ISBN 978-1-118-53534-9.

[11] D. Shen. Iterative learning control with incomplete information: A survey. *IEEE/CAA Journal of Automatica Sinica*, 5(5):885–901, 2018.

[12] J. Shi, F.-R. Gao, and T.-J. Wu. Robust design of integrated feedback and iterative learning control of a batch process based on a 2D Roesser system. *Journal of Process Control*, 15(8):907–924, 2005.

[13] H. F. Tao, W. Paszke, E. Rogers, H. Z. Yang, and K. Gałkowski. Iterative learning fault-tolerant control for differential time-delay batch processes in finite frequency domains. *Journal of Process Control*, 56:112–128, 2017.

[14] W. X. Tian, H. L. You, K. Gu, C. F. Zhang, and X. Z. Jia. Two-level nested control chart for batch process in the semiconductor manufacturing. *IEEE Transactions on Semiconductor Manufacturing*, 29(4): 399–410, 2016.

[15] Y. Q. Wang, F. R. Gao, and F. J. Doyle III. Survey on iterative learning control, repetitive control, and run-to-run control. *Journal of Process Control*, 19(10):1589–1600, 2009.

[16] Y. Q. Wang, T. Liu, and Z. Zhao. Advanced PI control with simple learning set-point design: Application on batch processes and robust stability analysis. *Chemical Engineering Science*, 71:153–165, 2012.

[17] J.-Y. Wei, H.-F. Tao, S.-L. Hao, W. Paszke, and K. Gałkowski. Output feedback based robust iterative learning control via a heuristic approach for batch processes with time-varying state delays and uncertainties. *Journal of Process Control*, 116:159–171, 2022.

[18] X. Wu, J.-H. She, L. Yu, H. Dong, and W.-A. Zhang. Contour tracking control of networked motion control system using improved equivalent-input-disturbance approach. *IEEE Transactions on Industrial Electronics*, 68(6):5155–5165, 2020.

[19] L. H. Xie. Output feedback H_∞ control of systems with parameter uncertainty. *International Journal of Control*, 63(4):741–750, 1996.